Non-Invasive Multi-Camera Gait Analysis System and Its Application to Gender Classification

DIEGO GUFFANTI[ID][1,2]**, ALBERTO BRUNETE**[ID][1]**, (Member, IEEE), AND MIGUEL HERNANDO**[ID][1]**, (Member, IEEE)**

[1]Centre for Automation and Robotics (CAR UPM-CSIC), Universidad Politécnica de Madrid, 28012 Madrid, Spain
[2]Carrera de Ingeniería Electromecánica, Universidad Tecnológica Equinoccial (UTE), 230208 Santo Domingo, Ecuador

Corresponding author: Diego Guffanti (d.guffanti@alumnos.upm.es)

ABSTRACT Objective: Most studies have conducted human gait analysis using expensive and invasive photogrammetric systems. The objective of this study was to demonstrate that non-invasive and cost-effective systems based on depth cameras may be able to retrieve relevant features of human gait patterns. We aimed to prove this by solving the problem of gait classification by gender. Methods: 81 participants (40 female and 41 male) walked at a self-selected speed across a 4.8-meter walkway. Gait data was recorded using multiple depth sensors. Analysis in time domain included joint excursions by gait phases, range of movement (ROM), central tendency and dispersion measures, spatial variables, and center of mass (COM) position. The spectral analysis included principal frequency, magnitude, and phase shift during walking. Only features with significant differences by gender were used to train a support vector machine (SVM) classifier. Results: A total of 108 features presented significant differences by gender (p<0.05). On this basis, the accuracy of the chosen model was 96.7%. Trunk rotation, trunk sway, knee abduction/adduction, and pelvic obliquity were the most differentiated between the groups. The COM position shown a significant difference by gender (p=0.0065) with 51.7% and 51.0% for men and women respectively. Women proved to have significantly shorter normalized step width than men (p=0.0472). Conclusion: The proposed method was able to retrieve most of human gait features correctly, including differences in gait pattern by gender. Significance: Depth cameras represent a cost-effective system that could be used for a deeper biomechanical human gait analysis.

INDEX TERMS Gender, gait analysis, joint, limb, machine learning.

I. INTRODUCTION

The kinematic variables of human gait have been widely analyzed using photogrammetric systems. Precision, conformability, usability, and transportability are factors that influence the choice of a gait analysis system [1]. Today, highly accurate photogrammetry systems are available, including Qualisys, STT Systems, Vicon, and Optitrack. Although these systems are highly accurate, they use invasive methods to determine gait pattern. Photogrammetry systems use reflective markers attached to the body. Furthermore, this kind of system represents a very large investment. Alternatively, a system based on depth cameras could be used, representing a cost-effective and non-invasive method. Several options of RGB-depth (RGBD) cameras and libraries can

perform skeletal tracking applications. Kinect (V1, V2), Intel Realsense (D415, D435, EUCLID), Orbbec (Persee, Astra, Astra Pro), and TVICO are among the most popular on the market. The software included in depth cameras can capture up to 25 joints at more than 30 frames per second. It represents a real advantage when implementing a non-invasive gait analysis system. These cameras have a short range of view. To solve this problem, we believe that the use of more than one camera could be a good approach. This process is called multiple camera calibration and has been applied by several authors including [2]–[5]. Camera calibration allows the signals of several sensors to be coupled together achieving a longer recording area. The ability of such sensors to retrieve relevant information has been widely studied. Specifically, the Kinect sensor has been used extensively. It has been used from in-home gait measurement [6], kinematic gait analysis [7] to classification of normal and pathological gait [8].

The associate editor coordinating the review of this manuscript and approving it for publication was Tao Zhou[ID].

Some studies have validated their use while others have not. For example, in [9], a review of 12 studies indicated good validity of Kinect sensors for only some spatiotemporal gait parameters. On the contrary, the same study shows poor validity for gait kinematic variables. Mentiplay *et al.* [10] concluded that Kinect V2 cannot accurately obtain the kinematic parameters of lower extremities. In contrast, Lamine *et al.* [11] concluded that with preliminary calibrations gait kinematics could be accurately evaluated in several joints. To validate the ability of RGBD sensors to obtain human gait data, the well-known difference associated with gender was used. A topic of interest in human gait analysis has been finding differences by gender, which now are well known. Kinematic features are among the most analyzed by gender [12], including spatiotemporal variables, range of movement (ROM), and center of mass (COM) excursions. Most research have concluded that significant differences are found in trunk sway, pelvic obliquity, hip abduction and abduction, and step width. Several studies have analyzed vertical center of mass (VCOM) excursions and horizontal center of mass (HCOM) excursions. These studies have used parts of the trunk segment as an estimated position of COM, but not the real COM. It should be noted that gait spectrum features in the frequency domain have been less analyzed by gender. Lee and Grimson [13] used magnitudes and phases of dominant frequency as features for identification and gender classification. That study used the magnitude as the amount of body movement (which could be a more accurate measure than ROM). Interestingly, it used the time delay between different regions in the body as the phase measure. Unfortunately, the study did not clearly explain the differences found by gender.

In this context, the present paper hypothesizes that non-invasive, cost-effective systems based on depth cameras may be able to retrieve relevant features of human gait patterns. We aimed to prove this by solving the problem of gait classification by gender. For this purpose, a large number of features of interest were analyzed, both in time and frequency domains. Analysis in the time domain included joint excursions by gait phases, ROM, central tendency and dispersion measures, normalized spatial variables, and COM position. The spectral analysis included principal frequency, magnitude, and phase shift during walking.

II. METHODS

A. PARTICIPANTS

Eighty-one healthy participants aged in their twenties (40 female and 41 male, Table 1) were recruited from Universidad Politecnica de Madrid. All participants were free of current injury that resulted in limitation of physical activity level. The inclusion criteria was based on young and similarly aged participants. We required the use of comfortable walking shoes, light colors, and loose-fitting clothes. We preferred the use of shorts and T-shirts (no dresses or skirts). Demographic details of age, height, weight, and body mass

TABLE 1. Demographics.

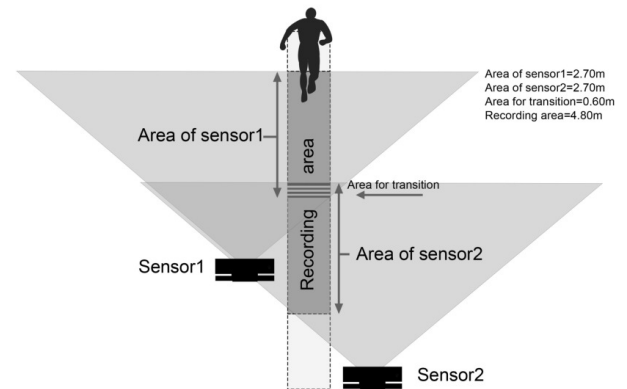|	Male (n=41) (mean $\pm$ SD)	Female (n=40) (mean $\pm$ SD)	p-value
Age (years)	22.3$\pm$3.4	21.5$\pm$3.8	p=0.3156
Height (m)	1.78$\pm$0.06	1.66$\pm$0.05	p<0.05
Weight (kg)	71.9$\pm$9.1	63.8$\pm$10.2	
BMI (kg/m^2)	22.8$\pm$2.7	23.1$\pm$3.4	p=0.6725

FIGURE 1. The Multi-Camera Git Analysis System configuration. The figure shows the range of view of each sensor and the total length of the effective recording area (4.8 meters). The overlaped field of view represents the area for transition between the segments.

index (BMI) were recorded for each participant. Significant differences were found between the male and female groups in height and weight (p<0.05 in both cases). There were no significant differences in age or BMI (p = 0.3156, 0.6725 respectively). Similarity in BMI indicates a similar body structure (in height–weight ratio) among the participants. On arrival at the laboratory, participants were familiarized with the experimental setup. After a static pose, each participant was asked to walk at a self-selected speed across a 4.8-meter walkway as in Fig. 1. This study was conducted according to the common standard guidelines of the Declaration of Helsinki.

B. DATA COLLECTION

1) OVERVIEW

Gait data based on 25 joint trajectories were recorded at 30 fps using two Kinect V2 depth sensors. When using a single-camera system, the captured data is not adequate to process information. It is because some samples at the beginning and end are unusable and disturbed (approximately 6 samples on each side). Therefore, we note that some studies keep the participant standing within the field of view of the camera and others prefer the use of treadmills. On the contrary we wanted to extend the range of view of the camera using a dual camera system.

There were other relevant details that led to the use of a dual-sensor system:

- The use of a single kinect sensor allows only one gait cycle to be retrieved with each foot. On the other hand, the use of two kinect sensors will detect between two and three gait cycles with each foot (Fig. 2).
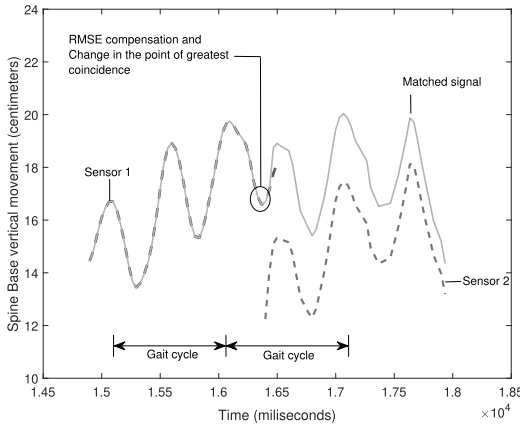
FIGURE 2. Matching process. The dotted lines represent the raw measurement from each sensor whereas the solid line is the result of the alignment of the data from sensor 2 with the data from sensor 1.

- By detecting at least two continuous gait cycles other gait pattern variables based on signal periodicity can be analyzed. It may include variables from the frequency spectrum.
- Two sensors are adequate to detect continuous gait cycles. The use of more sensors may result in repeated data, redundant information, as well as the use of large workspaces.

As is shown in Fig. 1, the general process involved placing the sensors one behind the other on each side of the walking path.

We ensure a common area where both cameras record the skeleton at the same time to smooth the transition between the signals. For the same reason that we mentioned earlier this common area had 12 unusable samples (6 at the end of sensor 1 and 6 at the beginning of sensor 2). It represents 50 centimeters of walkway at 30fps and 1.25 m/s (the average of pedestrian speed reported for both genders [14]). Therefore, we set a common area of 60 centimeters that was slightly higher than the minimum length. With this consideration, the total length of the effective recording area was 4.8 meters.

We synchronized the time base of both Kinect sensors by using a body gesture performed by support staff during data collection. A staff member stands inside the common area and raises their right hand. This gesture is recognized by both sensors as the starting signal for the timers. The data collection takes place after 10 seconds, once the support staff has has leaving the place and the participant is ready to start the test.

The recording process was well monitored and controlled by using a human–machine interface (HMI) developed in Visual Studio. The joints data were saved in real-time in a CSV file, which provided future analysis.

2) STEREO CALIBRATION
After setting up the sensors, we performed a stereo calibration which was required for transition between recorded segments. Camera calibration generally solves a set of unknown

parameters (intrinsic and extrinsic) based on the sensor projection process [15]. The intrinsic parameters are the focal length and the projection center of the camera. The extrinsic parameters are the rotation and translation matrix of the camera with respect to the reference. A widely used method is the checkerboard calibration algorithm proposed by Zhang in 1999 [16]. This method needs only a printed checkerboard, which provides simple operation and strong practicability. It has been widely used as a packaged toolbox function in multiple vision systems. We used the extrinsic parameters of the RGB camera as an approximation of depth camera. It is practical and effective.

The extrinsic parameters retrieved with the stereo calibration are as follows:

$$om = [-0.028\ 0.002\ 0.005] \pm [0.007\ 0.015\ 0.001] \quad (1)$$
$$T = [-1200.15\ -28.17\ -2062.8] \pm [7.86\ 6.17\ 16.4] \quad (2)$$

where om is the rotation vector measured in radians and T is the translation vector measured in milimeters. In the second part of each vector we can notice the numerical errors in the estimation of these vectors. These are the errors due to the calibration process.

All points sensed by the sensor 2 are transformed to the coordinate system of sensor 1 through the rigid motion transformation:

$$Sensor_1 = R * Sensor_2 + T \quad (3)$$

where R is the 3×3 rotation matrix corresponding to the rotation vector om. The relation between om and R is given by the Rodrigues formula [17].

In addition, we must compensate the offset that remains after applying the transformation matrix to the raw data from sensor 2. This process was implemented to smooth the transition between the signals. The offset is determined by calculating the root-mean-square error (RMSE) within the overlapped field of view. As mentioned above, the overlapped field of view is a common area where both sensors record the skeleton at the same time and using the same time base. We assert that since the time base of both Kinect sensors was synchronized as mentioned in the previous subsection. Therefore, the overlapped data can be retrieved based on timestamps. Once the overlapped data is found, the RMSE is calculated and it is added to all the transformed data from sensor 2.

Finally, we look for the point of greatest coincidence between these common frames to perform the transition between the signals. It is necessary to mention that this process is repeated for each axis in every joint trajectory. The matched signal in world coordinates had two or three gait cycles depending on the step length (Fig. 2).

3) SYSTEM ACCURACY
The final step was to measure the accuracy of the system with respect to the ground truth from a Vicon system.
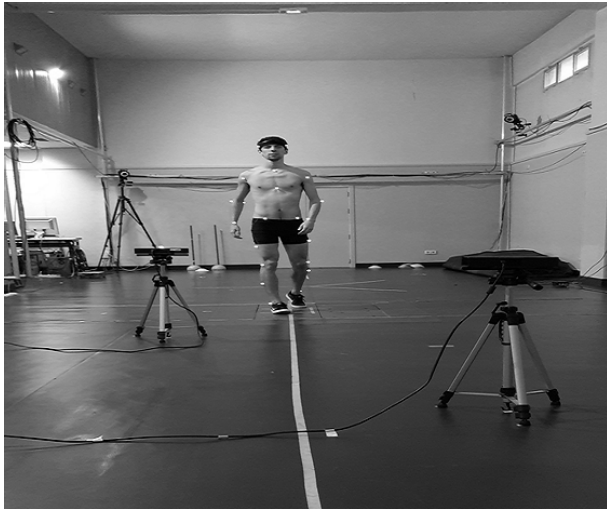
FIGURE 3. Workspace for comparison between Vicon and multiple depth sensors.

TABLE 2. NMAE error rate from the multiple kinect system w.r.t the Vicon system. Values are averaged for all iterations.

		NMAE (%) (mean±SD)	Pearson Correlation (mean±SD)
Sagittal	Knee	9.97 ± 2.28	0.9413±0.03
	Hip	7.80 ± 2.01	0.9551±0.02
	Shoulder	3.94 ± 2.77	0,9914±0.02
	Trunk	6.25 ± 4,03	0,9800±0.06
	Pelvis	10.18 ± 5.54	0,9318±0.09
Frontal	Knee	15.33 ± 7.71	0.7885±0.17
	Hip	14.99 ± 1.69	0.8439 ±0.15
	Shoulder	12.64 ± 2.88	0.9239±0.03
	Trunk	12.22 ± 3.70	0.8856±0.06
	Pelvis	13.61 ± 2.11	0.9271±0.06
Transverse	Trunk	12.60 ± 2.88	0,9427±0.07
	Pelvis	17.74 ± 2.06	0,9540±0.03

For this purpose, six Vicon M2 MCAM cameras with an opto-electric motion analysis system was used as the reference measure. Using the Vicon system, 3D locations of markers were recorded with a sampling rate of 120 Hz. With the collaboration of a test participant, six iterations were performed with both systems. The Fig. 3 shows the data collection environment in a real view.

Due to the difference in sampling frequencies the Vicon time series were linearly interpolated using the timestamps of Kinect data. This process ensures the same query points. Evidently, prior to this process, the signals from both systems needed to be synchronized in time. We did this using the starting point of the first gait cycle.

The error rates per joint and plane of joint kinematics angles are presented in Table 2. Pearson correlation demonstrates the similarity of both signals.

The metrics applied to measure the error rates were the Mean Absolute Error (MAE) and more specifically the Normalized Mean Absolute Error (NMAE). Given any gait measurement at timestamp t_i, the MAE error measures the average absolute deviation of Kinect signal k_i from the Vicon

signal v_i through the following formulae:

$$MAE = \frac{1}{N} \sum_{i=1}^{N} |k_i - v_i| \quad (4)$$

$$NMAE = \frac{MAE}{v_{max} - v_{min}} \quad (5)$$

where $v_{max} - v_{min}$ represents the angular range of movement (ROM) detected by the Vicon system in a specific joint.

In Fig. 4, the signals from all iterations were averaged to a single gait cycle to improve their presentation. Through Fig. 4 we can compare gait cycles retrieved from Vicon system and the multi-camera gait analysis system.

C. DATA ANALYSIS

From this point on, the proposed system was applied to the detection of differences in gait pattern by gender. We have chosen this application because we believe there is enough literature to compare the results we achieve.

In order to analyze gait, neighboring limbs were associated by the common joint, and the corresponding angles calculated. There were significant limitations in evaluating the ankle angle because it involved the toe coordinate, which had low accuracy with our depth sensor. Similar limitations have occurred in other studies, such as [11] or [18]. For this reason, we solely excluded the ankle angle from the analysis. The joint kinematics angles from the knee, hip, shoulder, trunk, and pelvis were performed for the sagittal and frontal planes. In addition, examination of the trunk and pelvis took place in the transverse plane. Using these angular signals, gait cycle, spectrum, and central tendency and dispersion features were performed for each plane. Normalized spatial variables and COM position and excursion were included in the analysis. Each gait sequence contains between two and three gait cycles depending on the step length. To analyze gait cycle phases, we averaged these cycles across the corresponding phases. On the contrary, to analyze spectrum features, central tendency and dispersion, spatial variables and the center of mass we used the entire signal. The sets of variables for analysis are described below.

1) GAIT CYCLE

Gait cycle analysis requires detecting the onset and the end of each cycle within the angular signal. For this purpose, we first defined the normalized cycles as described by Ceccato et al. [19]. We used the inter-ankle distance in the Z direction as the reference signal. The walking cycle was then defined by two successive peaks of the inter-ankle distance. These signal peaks were taken in the same direction (we used the up direction) and normalized from 0 to 100% of the gait cycle. Eight gait cycle phases were found during the stance and swing stages. Initial contact (IC-2%), loading response (LR-10%), mid stance (MSt-30%), terminal stance (TSt-50%), pre-swing (PSw-60%), initial swing (ISw-73%), mid swing (MSw-87%), and terminal swing (TSw-100%). The corresponding phases were averaged
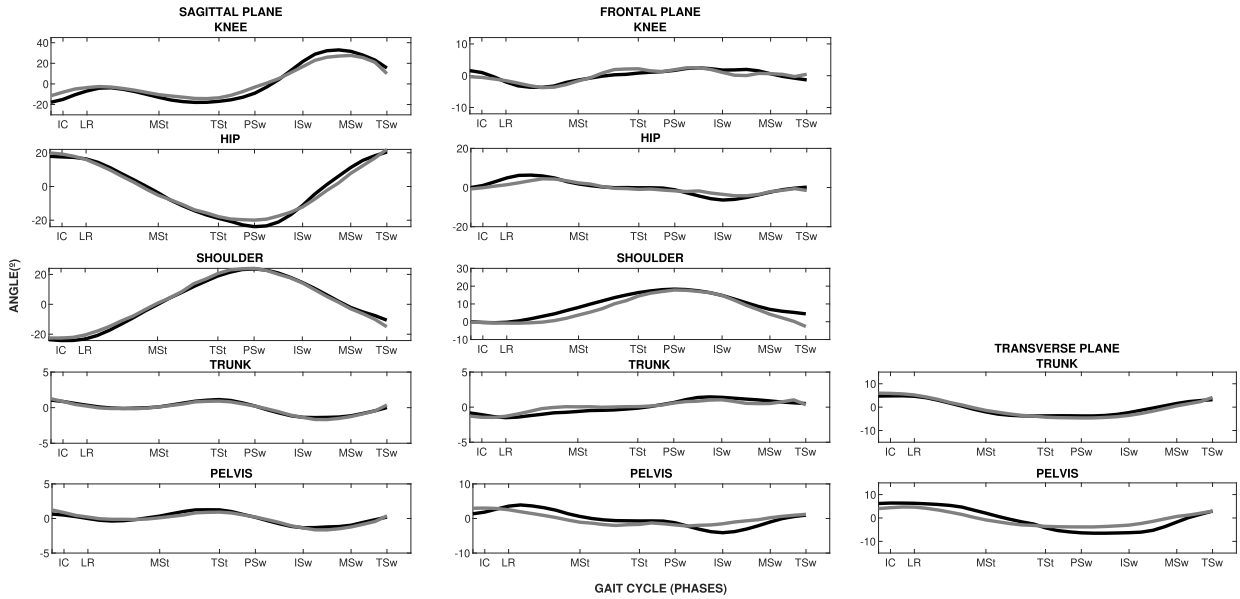
FIGURE 4. Comparison of gait cycles retrieved from Vicon system (black line) and the multi-camera gait analysis system (gray line) in sagittal, frontal, and transverse planes. Eight gait cycle phases are shown in each plot: initial contact (IC-2%), loading response (LR-10%), mid stance (MSt-30%), terminal stance (TSt-50%), pre-swing (PSw-60%), initial swing (ISw-73%), mid swing (MSw-87%), and terminal swing (TSw-100%).

within all gait cycles found for the same participant. It is between two and three gait cycles per participant depending on the step length. In addition, the ROM was performed to evaluate the amount of movement around each specific joint.

2) SPECTRUM
Spectrum features were retrieved using the Signal Processing Toolbox from Matlab R2018b (MathWorks Inc, Natick, MA). The spectral analysis was performed to include features that allow us to analyze gait as a periodic signal. Principal frequency (Pfrec) represented the frequency with the highest magnitude in the spectrum. The magnitude of principal frequency (Pmag) can be understood as the amount of motion that occurs periodically at the principal frequency. Phase shift at principal frequency (Pphase) was a special feature to measure the harmony of walking. Harmony of walking represented the quality of coordination between joints excursions. Phase cannot be directly used because each gait sequence is not predetermined to start at a particular point of a walking cycle. For this reason, the phase shift of the joints was computed in relation to one particular signal. This signal was the "most stable"; in our case, the standard phase was that of the inter-ankle distance.

3) CENTRAL TENDENCY AND DISPERSION
Central tendency and dispersion measures were retrieved from angular signals in the time domain. These features are useful to understand the tendencies of people to carry their joints in different ways. For this reason, the mean position, Q25 quartile, Q75 quartile, and interquartile range (IQR) were used as statistical descriptors of structural differences.

In addition, signal entropy was included in the analysis because it has been widely used for abnormal gait detection and analysis [20]–[22]. Entropy has been used as an index to quantify the complexity, disorder, and irregularities of time series. Therefore, entropy was included in the analysis.

4) SPATIAL VARIABLES
Spatial variables were calculated and non-dimensionalized. Step and stride length were normalized by leg length according to [23]. Step width was normalized to hip width according to [24]–[26].

5) CENTER OF MASS
The analysis of COM was implemented based on the Winter method [27]. The body segment parameters described in Table 3 were used for COM calculation.

The coordinates of the proximal and distal ends of nine body segments were found (trunk, head, neck, thighs, feet, legs, upper arms, forearms, and hands). The COM of each body segment was defined using the following formulae:

$$x_{CM} = x_p I_p + x_d I_d \tag{6}$$
$$y_{CM} = y_p I_p + y_d I_d \tag{7}$$

where the x_{CM} and y_{CM} are the coordinates of COM in one segment. The x_p and y_p are the coordinates of the proximal end. The x_d and y_d are the coordinates of the distal end. In addition, I_p and I_d are the percentages of segmental length from the proximal and distal ends, respectively. Total COM is the weighted average of the calculated COM of the nine

TABLE 3. The body segment parameters adapted from Winter [27] for COM calculation.

Body segment	Segment definitions		Segment mass (m)/	CM/segment length	
	Proximal end	Distal end	total body mass(M)	Proximal	Distal
Trunk-head-neck	Head	Spine-base	0.578	0.660	0.340
Thighs	Hip	Knee	0.100	0.433	0.577
Feet and legs	Knee	Ankle	0.061	0.606	0.394
Upper arms	Shoulder	Elbow	0.028	0.436	0.564
Forearms and hands	Elbow	Wrist	0.022	0.682	0.318

segments, calculated using the formulae:

$$x_{COM} = \frac{\sum_{n=1}^{9} m_i x_i}{M} \quad (8)$$

$$y_{COM} = \frac{\sum_{n=1}^{9} m_i y_i}{M} \quad (9)$$

where the x_{COM} and y_{COM} are the coordinates of total COM. The x_i and y_i are the coordinates of the i-th segment. The m_i is the mass of the i-th segment, and M is the body mass of the n segments. Based on these results, VCOM and HCOM excursions were performed during all gait cycles. In addition, the body position of COM normalized with respect to the height of each participant.

D. MACHINE LEARNING CLASSIFIER

Five groups of features were built, with a total of 222 features for each participant. We used an 81×222 matrix, where rows represent the number of participants and columns the number of features. From the original 81 observations, 61 were found to be valid (30 female and 31 male observations). The remainder was discarded due to the presence of signal discontinuities that caused unusable information. A two-sample t-test was used to detect the significance level of each feature. Statistical significance was defined as a p-value of less than 0.05. Only features with statistically significant differences were chosen to train the classification model. For this purpose, we used the Classification Learner app, a Machine Learning Toolbox from Matlab R2018b (MathWorks Inc, Natick, MA).

III. RESULTS

The proposed system was employed to test the ability of depth cameras to retrieve human gait features. We addressed this by solving the problem of classification of gait by gender. Some differences found in gait pattern by gender support earlier theories where certified devices were used.

A. GAIT CYCLE, SPECTRUM AND CENTRAL TENDENCY AND DISPERSION

Results of this set of variables are shown in Table 4.

Knee. In the sagittal plane, during IC, the limb was positioned to start stance phase using the heel as a rocker. The curve described in Fig. 5 shows that in this phase the knee is slightly flexed. In LR, knee flexion is increased for shock absorption because the body weight is transferred onto the limb. Then, during the rest of MSt, the knee is gradually extended. No significant differences were found in these latter phases. Women continued knee extension until the end of TSt.

In contrast, men started a slight knee flexion, a significant difference (p = 0.0046). During PSw, where the floor contact by the opposite limb has started, the knee responds with increased flexion. The knee reached maximum flexion at the end of ISw (without differences by gender), when the foot is lifted. Finally, in MSw, the knee was extended in response to gravity and continued extending until the end of TSw (without differences by gender in both cases).

An interesting difference was found in the frequency domain for the phase shift of knee flexion (p = 0.015). Women delay knee flexion and therefore foot lift. Women tried to reach a more extended position before starting the swing phase. This is associated with anatomical differences; these differences showed women have shorter legs than men. For this reason, women tried to increase their knee extension to reach a higher advance with the forward limb. In the frontal plane, significant differences were found during LR (p = 0.0316) and more pronounced in MSt (p = 0.0003) where women had a higher knee abduction (Fig. 5). It is the response to limb loading that moves the whole body nearer to the supporting foot. Conversely, men carried their knees in a slight adduction. During TSt and PSw, the knee is adducted because the load on the limb is removed as the floor contact by the other limb has started. No significant differences were found in these phases. Finally, during the swing, the knee returned to a more neutral posture with significant differences in ISw, MSw, and TSw (p<0.05 in all cases). During these phases, men continued with a higher knee adduction than women. Accordingly, in the frontal plane, women demonstrated a higher ROM and IQR value than men (p = 0.0002, 0.0168, respectively). In addition, women demonstrated a smaller mean position and Q25 quartile value (p = 0.0194, 0.0009, respectively). This suggests a more abducted knee angle for women during the gait cycle. Another significant difference was found in the signal entropy of knee excursion in the frontal plane (p = 0.00004), with a higher value for women than men.

Hip. The results showed that women had greater hip ROM in the sagittal plane (p = 0.0035). This was associated with greater hip extension during TSt (p = 0.0128) and greater flexion (p = 0.0425) during MSw. Due to the anatomical angle between femur and tibia, hips were kept in an adducted position. This occurred mainly during the onset of stance and ending of swing phases, with significant differences (p<0.05). A relative hip abduction existed only during the ending of stance phase, without significant differences. Furthermore, during the full gait cycle, women carried their hips

TABLE 4. Means, standard deviations, and p-values of three groups of variables: gait cycle, spectrum, and central tendency and dispersion of knee, hip, shoulder, trunk, and pelvis excursion in three planes: sagittal, frontal, and transverse. Gender differences were evaluated with two-sample t-test, and p-values less than 0.05 represent significant differences.

		Knee (mean ± SD)			Hip (mean ± SD)			Shoulder (mean ± SD)			Trunk (mean ± SD)			Pelvis (mean ± SD)		
		Men	Women	p-value	Men	Women	p-value	Men	Women	p-value	Men	Women	p-value	Men	Women	p-value
								Sagittal plane								
1	IC (°)	3.4 ± 6.9	3.6 ± 10.8	0.9295	21 ± 4.7	22.4 ± 5.4	0.2782	-13.5 ± 5.9	-12.2 ± 7.2	0.4477	3.9 ± 2	2.2 ± 1.6	0.0004	3.2 ± 2	1.5 ± 1.6	0.0003
2	LR (°)	7.3 ± 7.6	6.4 ± 10.6	0.7028	17.9 ± 5.1	19.2 ± 5.9	0.3534	-12.7 ± 6.1	-11.8 ± 7.6	0.6095	3 ± 2.1	1.5 ± 1.5	0.0021	2.2 ± 2.1	0.7 ± 1.5	0.0020
3	MSt (°)	2.7 ± 6.9	5.3 ± 8.7	0.2133	-7.2 ± 5.5	-4.6 ± 5.3	0.0579	0.3 ± 6.3	-1.7 ± 6.2	0.2181	1.7 ± 1.9	0.6 ± 1.8	0.0291	0.9 ± 1.9	-0.1 ± 1.7	0.0279
4	TSt (°)	4.4 ± 7.3	-1.1 ± 7.4	0.0046	-19.8 ± 4.9	-22.6 ± 3.5	0.0128	11.1 ± 7.5	10.1 ± 6.6	0.5925	3.7 ± 1.6	2.1 ± 1.8	0.0005	3 ± 1.6	1.4 ± 1.7	0.0004
5	PSw (°)	17.2 ± 9.4	14.3 ± 8	0.1904	-18.8 ± 5.1	-20.5 ± 4.1	0.1520	7.9 ± 6.6	7.7 ± 6.4	0.8816	2.8 ± 1.8	1.4 ± 1.7	0.0048	2 ± 1.8	0.7 ± 1.7	0.0050
6	Isw (°)	37.2 ± 4.4	39.1 ± 6.3	0.1662	-4.6 ± 6.4	-4.1 ± 5.4	0.7615	-1.3 ± 4.4	-0.9 ± 4.8	0.6942	1.4 ± 1.8	0.3 ± 1.6	0.0153	0.7 ± 1.8	-0.4 ± 1.6	0.0157
7	MSw (°)	28 ± 10.9	33.5 ± 10.6	0.0501	14.1 ± 5.3	16.8 ± 4.8	0.0425	-10.2 ± 4.3	-9.3 ± 5.8	0.5148	2.4 ± 1.9	1.2 ± 1.7	0.0093	1.7 ± 1.9	0.4 ± 1.7	0.0095
8	TSw (°)	9.1 ± 6.9	7.4 ± 9.9	0.4211	20.5 ± 3.8	21.9 ± 4.2	0.1681	-13.8 ± 5.5	-12.9 ± 6.7	0.5649	3.1 ± 1.8	1.7 ± 1.7	0.0023	2.4 ± 1.8	1 ± 1.7	0.0020
9	ROM (°)	39.3 ± 5	43.3 ± 6	0.0068	42.5 ± 5.2	46.2 ± 4.2	0.0035	26 ± 10.2	24.5 ± 10.3	0.5488	3.1 ± 0.8	2.9 ± 1	0.2259	3.1 ± 0.8	2.8 ± 1	0.1903
10	Pfrec (Hz)	0.8 ± 0.3	0.8 ± 0.2	0.5278	0.9 ± 0.1	0.9 ± 0.04	0.3291	0.9 ± 0.1	0.9 ± 0.1	0.5984	1.8 ± 0.1	1.7 ± 0.3	0.0558	1.8 ± 0.1	1.7 ± 0.3	0.0539
11	Pmag (DB)	22.7 ± 3.2	21.9 ± 1.6	0.2559	23.4 ± 1	23.9 ± 0.9	0.0566	18.7 ± 3.5	17.5 ± 4.1	0.2211	-0.4 ± 1.8	-2.9 ± 2.6	0.0001	-0.4 ± 1.7	-3 ± 2.6	0.0000
12	Disphase(rad)	1.4 ± 0.3	1.2 ± 0.3	0.0150	0.05 ± 0.04	0.06 ± 0.04	0.3598	2.9 ± 0.2	2.9 ± 0.2	0.8135	0.4 ± 0.3	0.5 ± 0.4	0.3796	0.4 ± 0.3	0.4 ± 0.4	0.3735
13	Mean position (°)	13 ± 4.2	12.5 ± 7.9	0.7279	-0.2 ± 3.6	-0.02 ± 3.7	0.8724	-2.3 ± 3.7	-2.8 ± 4.9	0.6560	2.5 ± 1.7	1.3 ± 1.5	0.0052	1.8 ± 1.7	0.6 ± 1.5	0.0050
14	Q25 (°)	1.4 ± 4.4	-0.03 ± 7.8	0.3709	-14.5 ± 4	-15.1 ± 3.8	0.5262	-11.6 ± 4.8	-11 ± 6.1	0.6748	1.4 ± 1.8	0.3 ± 1.5	0.0060	0.7 ± 1.8	-0.5 ± 1.4	0.0059
15	Q75 (°)	25.2 ± 5.2	24.6 ± 9.2	0.7326	15.4 ± 3.9	16.1 ± 4.7	0.5829	6.4 ± 5.4	4.9 ± 6.1	0.3048	3.7 ± 1.7	2.3 ± 1.7	0.0033	2.9 ± 1.7	1.6 ± 1.7	0.0032
16	IQR (°)	23.8 ± 4.6	24.6 ± 6.1	0.5673	29.9 ± 3.7	31.2 ± 3.7	0.1967	18 ± 7.4	15.8 ± 6.8	0.2496	2.2 ± 0.5	2.1 ± 0.6	0.2937	2.2 ± 0.5	2 ± 0.6	0.2874
17	Entropy (n/a)	3.9 ± 0.2	4 ± 0.2	0.0920	3.9 ± 0.1	4 ± 0.1	0.0071	3.4 ± 0.4	3.4 ± 0.4	0.7104	1.7 ± 0.2	1.7 ± 0.3	0.1417	1.7 ± 0.2	1.6 ± 0.3	0.1419
								Frontal plane								
1	IC (°)	2.4 ± 5.8	-0.7 ± 7.3	0.0665	-1.4 ± 4.3	1.7 ± 4.3	0.0053	11.7 ± 4.9	8.1 ± 3.4	0.0013	-1.4 ± 1.4	-0.2 ± 1.5	0.0024	2.1 ± 1.6	2.9 ± 1.8	0.0625
2	LR (°)	3.1 ± 5.4	-0.4 ± 6.8	0.0316	-1 ± 4.2	2 ± 4.3	0.0072	11.3 ± 4.2	7.9 ± 3.6	0.0010	-1.9 ± 1.5	-0.6 ± 1.5	0.0012	2.3 ± 1.7	2.7 ± 2	0.4244
3	MSt (°)	2.4 ± 6.8	-4.4 ± 7.2	0.0003	-0.4 ± 3.3	3.5 ± 4	0.0001	11.4 ± 3.8	9.3 ± 3.3	0.0225	-0.9 ± 1.4	0 ± 1.4	0.0147	-1.6 ± 1.8	-1.7 ± 1.6	0.7944
4	TSt (°)	8.4 ± 6	8.8 ± 4.9	0.7791	-4.1 ± 3.2	-3.6 ± 3.2	0.5018	15.6 ± 4.3	12.2 ± 3.6	0.0013	-0.6 ± 1.5	-0.1 ± 1.1	0.1596	-2.3 ± 1.3	-2.4 ± 1.5	0.6935
5	PSw (°)	7.6 ± 7.7	7.5 ± 4.7	0.9570	-3.4 ± 3.6	-3.1 ± 3.6	0.7202	14.4 ± 4	11.9 ± 4.2	0.0195	0.2 ± 1.4	0.4 ± 1.2	0.4957	-2.2 ± 1.3	-2.5 ± 1.3	0.3179
6	Isw (°)	6.6 ± 4.4	2.7 ± 4.5	0.0012	-2.2 ± 2.6	-0.3 ± 2.4	0.0039	12.1 ± 3.2	9.4 ± 2.9	0.0009	0.4 ± 1.2	0.6 ± 1.3	0.5433	-0.1 ± 1.4	0.1 ± 1.3	0.7080
7	MSw (°)	3.7 ± 3.7	0.2 ± 5	0.0025	-1.5 ± 2.7	0.1 ± 2.9	0.0272	12.4 ± 3.7	9.1 ± 2.4	0.0001	-0.04 ± 1.2	0.1 ± 1.2	0.5579	1.5 ± 1.2	1.6 ± 1.4	0.6181
8	TSw (°)	2.2 ± 4.2	-0.4 ± 5.4	0.0357	-0.9 ± 3.2	1.3 ± 3.4	0.0094	12.6 ± 4	9 ± 3.2	0.0002	-0.7 ± 1.3	-0.04 ± 1.2	0.0432	1.5 ± 1.5	2.3 ± 1.5	0.0563
9	ROM (°)	10.8 ± 4.4	15.5 ± 5	0.0002	7 ± 2.8	8.8 ± 3	0.0156	7.3 ± 3.5	7 ± 4.4	0.7310	2.9 ± 1.2	2.4 ± 0.8	0.0360	5.6 ± 0.8	6.5 ± 1.3	0.0058
10	Pfrec (Hz)	0.6 ± 0.3	0.7 ± 0.4	0.1814	0.6 ± 0.3	0.7 ± 0.5	0.2541	0.8 ± 0.5	0.8 ± 0.4	0.9263	0.8 ± 0.4	0.5 ± 0.3	0.0139	0.8 ± 0.3	0.7 ± 0.3	0.6504
11	Pmag (DB)	11.4 ± 6.3	13.6 ± 3.1	0.0861	8.6 ± 3.1	9.1 ± 3.5	0.5618	6.4 ± 4.7	6 ± 5.2	0.7495	0.01 ± 3.6	-1.1 ± 3	0.1977	6.2 ± 2.6	6.2 ± 2.5	0.9955
12	Disphase(rad)	2.5 ± 0.4	2.5 ± 0.4	0.7067	1 ± 0.8	0.9 ± 0.7	0.6347	2.2 ± 1	2.2 ± 0.9	0.8122	1.7 ± 0.7	1.6 ± 1	0.6747	0.3 ± 0.3	0.3 ± 0.3	0.9181
13	Mean position (°)	4.4 ± 4.4	1.5 ± 5	0.0194	-1.5 ± 2.4	0.4 ± 3	0.0071	12.8 ± 3.3	9.8 ± 2.6	0.0003	-0.7 ± 1	-0.1 ± 1	0.0222	-0.04 ± 1	-0.1 ± 1.3	0.8711
14	Q25 (°)	1.3 ± 4.3	-3.1 ± 5.5	0.0009	-3.8 ± 2.5	-2.4 ± 2.6	0.0317	10.3 ± 3.3	7.2 ± 2.9	0.0003	-1.7 ± 1.2	-0.9 ± 1	0.0066	-1.9 ± 1.1	-2 ± 1.2	0.7675
15	Q75 (°)	7.7 ± 4.4	5.8 ± 5.7	0.1699	0.9 ± 2.5	3.5 ± 3.5	0.0012	15 ± 3.6	12.4 ± 3.2	0.0039	0.3 ± 1	0.7 ± 1.1	0.1113	2 ± 1.1	1.9 ± 1.4	0.7897
16	IQR (°)	6.4 ± 3.1	9 ± 4.9	0.0168	4.7 ± 1.6	5.9 ± 2.4	0.0225	4.7 ± 2.2	5.1 ± 2.8	0.4810	2 ± 0.8	1.6 ± 0.5	0.0281	3.9 ± 0.8	3.9 ± 1	0.9888
17	Entropy (n/a)	2.8 ± 0.3	3.2 ± 0.3	0.0000	2.5 ± 0.2	2.7 ± 0.2	0.0016	2.3 ± 0.4	2.4 ± 0.4	0.3113	1.5 ± 0.3	1.4 ± 0.2	0.1892	2.2 ± 0.2	2.2 ± 0.2	0.2023
								Transverse plane								
1	IC (°)	-	-	-	-	-	-	-	-	-	8.1 ± 2.8	11.6 ± 4	0.0002	8.4 ± 3.3	11 ± 4.6	0.0126
2	LR (°)	-	-	-	-	-	-	-	-	-	7.7 ± 2.7	10.9 ± 4.1	0.0005	8.3 ± 3	10.8 ± 4.6	0.0154
3	MSt (°)	-	-	-	-	-	-	-	-	-	2.7 ± 2.8	5.9 ± 3.5	0.0002	5.2 ± 2.8	7.2 ± 4.3	0.0365
4	TSt (°)	-	-	-	-	-	-	-	-	-	0.3 ± 2.7	2.6 ± 3	0.0022	3 ± 2.8	4 ± 3	0.2123
5	PSw (°)	-	-	-	-	-	-	-	-	-	0.3 ± 2.7	3.1 ± 2.9	0.0002	2.8 ± 2.6	4.4 ± 3.3	0.0397
6	ISw (°)	-	-	-	-	-	-	-	-	-	2.9 ± 3.1	5.7 ± 2.8	0.0006	4 ± 3	6.1 ± 3.2	0.0106
7	MSw (°)	-	-	-	-	-	-	-	-	-	6.1 ± 3	9.2 ± 3.2	0.0002	6.5 ± 3.2	9.3 ± 3	0.0006
8	TSw (°)	-	-	-	-	-	-	-	-	-	7.2 ± 2.8	10.1 ± 3.2	0.0003	7.4 ± 2.9	10.3 ± 3	0.0004
9	ROM (°)	-	-	-	-	-	-	-	-	-	8.4 ± 2.7	9.7 ± 3.3	0.1041	6.6 ± 2.3	8.1 ± 3.6	0.0504
10	Pfrec (Hz)	-	-	-	-	-	-	-	-	-	0.8 ± 0.2	0.9 ± 0.1	0.1506	0.6 ± 0.3	0.8 ± 0.2	0.0022
11	Pmag (DB)	-	-	-	-	-	-	-	-	-	9.2 ± 2.9	10 ± 2.9	0.2631	7 ± 3.1	8.4 ± 3.5	0.0907
12	Disphase(rad)	-	-	-	-	-	-	-	-	-	0.3 ± 0.2	0.3 ± 0.3	0.6031	0.4 ± 0.3	0.4 ± 0.3	0.8920
13	Mean position (°)	-	-	-	-	-	-	-	-	-	4 ± 2.5	7 ± 2.8	0.0000	5.9 ± 2.6	8 ± 3.4	0.0101
14	Q25 (°)	-	-	-	-	-	-	-	-	-	1 ± 2.7	3.9 ± 2.8	0.0001	3.5 ± 2.6	5.1 ± 3.2	0.0470
15	Q75 (°)	-	-	-	-	-	-	-	-	-	6.8 ± 2.7	10 ± 3.2	0.0001	8.1 ± 2.8	10.9 ± 3.5	0.0011
16	IQR (°)	-	-	-	-	-	-	-	-	-	5.8 ± 2.1	6.1 ± 1.8	0.5265	4.6 ± 1.3	5.8 ± 1.8	0.0032
17	Entropy (n/a)	-	-	-	-	-	-	-	-	-	2.4 ± 0.3	2.6 ± 0.3	0.0086	2.4 ± 0.3	2.5 ± 0.3	0.01128

in greater adduction than men. This measure was confirmed by the mean, Q25, and Q75 features (p<0.05 in all cases). This means that women carried their legs towards the midline of the body. This could have influenced the step width, where women showed a smaller normalized value than men (p = 0.0472). Another significant difference was found in signal entropy in the sagittal (p = 0.0071) and frontal planes (p = 0.0016), with a higher value for women than men. Hip movement in the transverse plane was not analyzed, due to sensor limitations. Finally, no significant differences were found in frequency features for the hip joint.

Shoulder. There were no significant differences for shoulder ROM in either the sagittal or frontal plane. Surprisingly, differences in shoulder mid-position in the frontal plane were found. This is notable in the curve analysis (Fig. 5). Mean, Q25, and Q75 (p<0.05 in all cases) showed that women kept their arms more attached to the body.

Trunk and pelvis. The sagittal angle of the trunk and pelvis followed a double sinusoidal path as shown in the curve analysis (Fig. 5). Peaks of flexion occurred in the onset of LR and during PSw, periods of double limb support. Each extension occurred in the two single support intervals: the
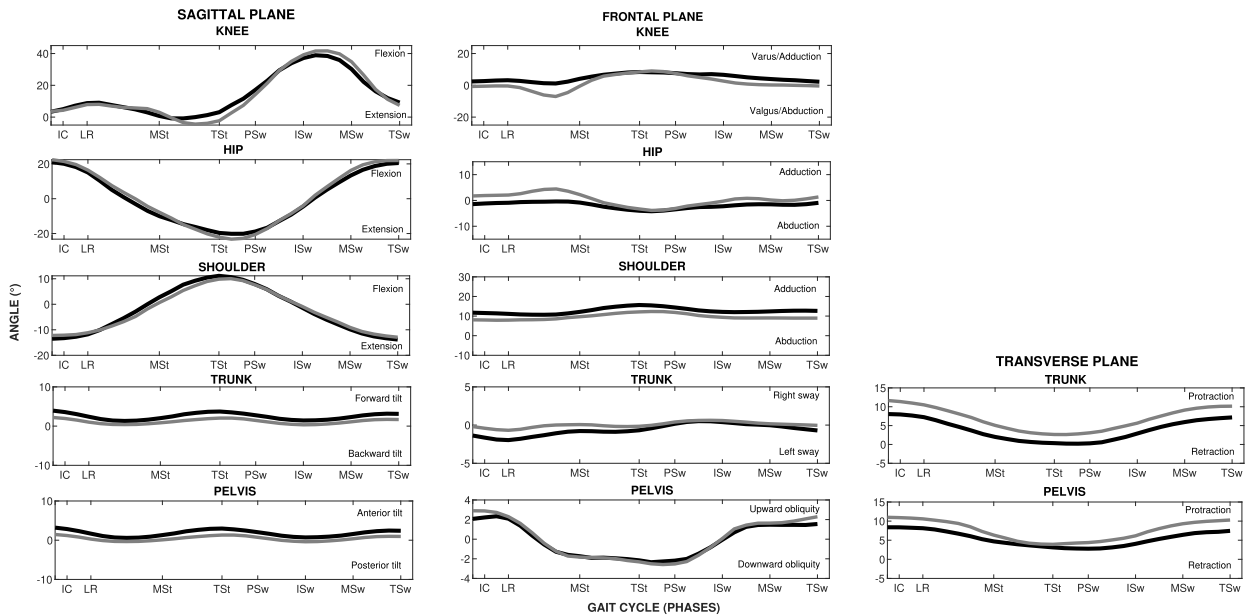
FIGURE 5. Gait cycles for men (black line) and women (gray line) in sagittal, frontal, and transverse planes with values averaged by gender in corresponding points (phases). Eight gait cycle phases are shown in each plot: IC-2%, LR-10%, MSt-30%, TSt-50%, PSw-60%, ISw-73%, MSw-87%, TSw-100%.

onset of TSt and MSw. During these movements, trunk and pelvis had similar results. Both presented significant differences by gender in whole gait phases and most central tendency measures such as mean, Q25, and Q75 (p<0.05 in all cases). Obviously, there is a structural difference rather than a kinematic difference. This showed that men maintain a greater average natural forward tilt than women. When we analyzed ROM or IQR measures, no significant differences were found. However, when we analyzed the magnitude of principal frequency, a significant difference could be found. In the sagittal plane, men exceed women by 2.5 dBs for trunk (p = 0.0001) and 2.6 dBs for pelvis (p = 0.00003). This means a greater movement of 33% and 35% for trunk and pelvic tilt respectively. The differences in the frequency spectrum can be observed in the Fig. 6 where the principal frequency is circled for each graph.

In the frontal plane, for trunk sway and pelvic obliquity, the path was a single sinusoid for each gait cycle (Fig. 5). The signal had a progressive angle toward the side of the supporting limb. In trunk sway, significant differences were found in the onset of stance phases and the last swing phase (p<0.05 in all cases). Additionally, the results showed that men had higher side-to-side trunk sway frequency (p = 0.0139). Men also had greater ROM and IQR measures (p = 0.036, 0.0281 respectively), whereas women presented higher pelvic obliquity. Another difference was found in the Q25 measure, which showed that the main differences in trunk sway were in the first half of the gait cycle. Finally, there was a significant difference in mean position for trunk sway, with a greater value for men than women. This showed that women carry their trunk more centered, whereas men try to lean their body sideward. In the transverse plane, there

were significant differences for trunk and pelvic rotation (protraction–retraction) in central tendency measures. Mean, Q25, and Q75 (p<0.05 in all cases) showed a difference in mid-rotation, with greater values for women than men. This is notable in the curve analysis (Fig. 5). Again, there is a structural difference rather than a kinematic difference. This means that women and men took different strategies for trunk and pelvic rotation. Women tried to increase protraction and decrease retraction of the trunk and pelvis. As discussed earlier, this could be a strategy to compensate leg advance for the fact that women have shorter legs than men. Differences in whole gait phases were related to the difference in mid-position. Additionally, results showed that women had higher pelvic rotation frequency (p = 0.0022) and a greater IQR measure (p = 0.0032). Despite the fact that women had greater ROM for trunk rotation than men, this value was not significant. We found significant differences in entropy measures for trunk and pelvic rotation (p<0.05 in all cases), with higher values for women than men.

B. CENTER OF MASS
The COM position, implemented based on [27], showed an interesting anatomical difference by gender. We performed the COM position normalized with respect to the height of each participant. The results (Table 5) showed that men had a COM position higher than women. Men had a COM position at 51.7% of their body height, and women at 51.0% of their body height, a statistically significant difference (p = 0.0065). This could be because anatomically, women have shorter legs than men, which moves their COM position down. Additionally, no significant differences were found for VCOM or HCOM excursions.
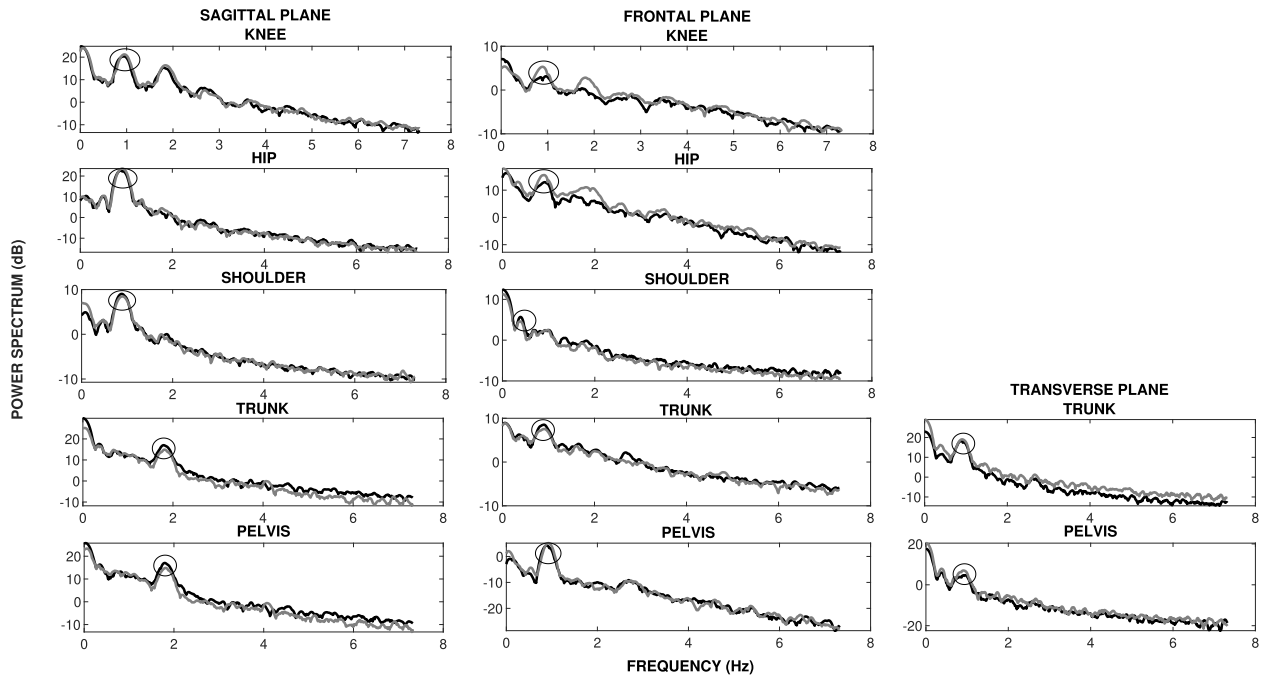
FIGURE 6. Power Spectrum from joint kinematic angles for men (black line) and women (gray line) in sagittal, frontal, and transverse planes. The values were averaged by gender in corresponding frequencies. Principal frequency (Pfrec) is circled for each graph and represents the frequency with the highest magnitude in the spectrum.

TABLE 5. Means, standard deviations, and p-values of COM excursions. Body segment parameters were adapted from Winter [27] for COM calculation. The variable "body position" shows the position of COM normalized with respect to the height of each participant. The horizontal (HCOM) and vertical (VCOM) excursions were calculated during each gait cycle and then averaged. Gender differences were evaluated with two-sample t-test, and p-values less than 0.05 represent significant difference.

COM			
	Male (mean±SD)	Female (mean±SD)	p-value
Body position(%)	51.7±1.1	51±0.9	0.0065
HCOM(cm)	3±0.9	3.1±0.9	0.6060
VCOM(cm)	3.3±1.1	3.1±0.7	0.4761

TABLE 6. Means, standard deviations, and p-values of spatial parameters: step length, stride length, and step width. Gender differences were evaluated with two-sample t-test, and p-values less than 0.05 represent significant differences.

Spatial features			
	Male (mean±SD)	Female (mean±SD)	p-value
Step length(cm)	0.67±0.09	0.7±0.07	0.1866
Stride length(cm)	1.35±0.15	1.38±0.15	0.4577
Step width(cm)	0.42±0.09	0.37±0.08	0.0472

C. SPATIAL FEATURES

Women had significantly shorter normalized step width than men (p = 0.0472). It was the result of greater hip adduction and higher knee abduction during the gait cycle. For this reason, women carried their legs towards the midline of the body more than men. In addition, step and stride length normalized by leg length were retrieved. Although women had longer normalized step and stride length than men, no significant differences were found by gender (Table 6).

D. MACHINE LEARNING CLASSIFIER

A total of 222 features were retrieved for each participant. The matrix of features had a dimension of 81 × 222, where rows represented the number of participants and columns the number of features. As mentioned above, from the original 81 observations, 61 were found to be valid (30 female and 31 male observations). The remainder was discarded due to the presence of signal discontinuities that caused unusable information. Then, a two-sample t-test was used to detect the significance level of each feature. In this context, only 108 features presented significant differences by gender (p<0.05). These features were used to train a machine learning classifier. Therefore, the size of the final training matrix was 61 × 108.The selected model was an SVM that used the quadratic kernel for classification between classes. A four-fold cross-validation was applied, and results are reported through a confusion matrix (Fig. 7) and ROC curve (Fig. 8).

In Fig. 7, 1 represents the positive female class and 2 the negative male class. TP, FN, FP and TN represent the number of true positives, false negatives, false positives and true negatives, respectively. N represents the number of observations. The accuracy (ACC) can be defined as the percentage of correctly classified instances. It was calculated as follows:

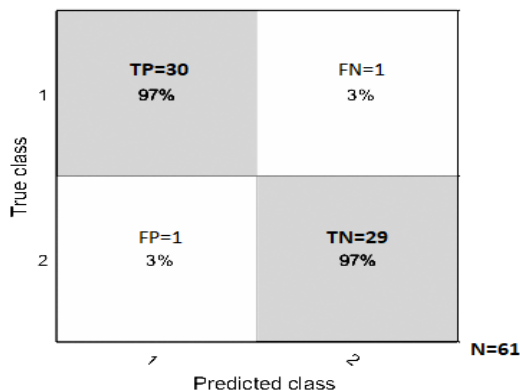$$ACC = \frac{TP + TN}{TP + TN + FP + FN} = 96.7\% \qquad (10)$$

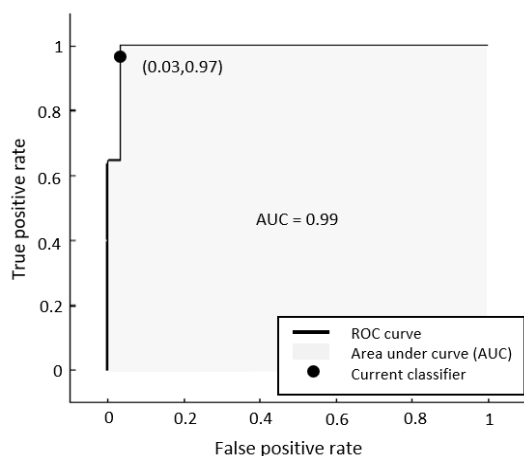FIGURE 7. Confusion matrix, 1 represents the positive female class and 2 the negative male class.
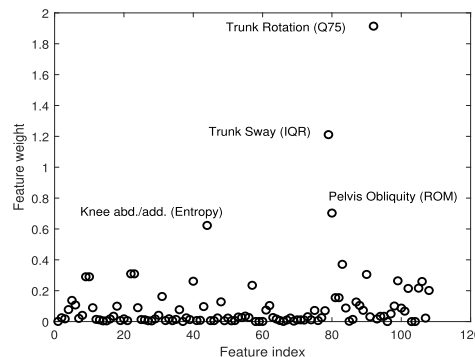

FIGURE 9. Significant differences weighted with the multivariate NCA algorithm. The highlighted features are labeled in the scatter plot.

knee abduction and adduction (entropy), and pelvic obliquity (ROM) were the features most differentiated between the groups.

IV. DISCUSSION

Kinematic comparisons by gender have been primarily analyzed using discrete joint angle metrics, with ROM the most frequently reported variable in the literature. Some additional variables are the mean, maximum, or minimum values of excursions during the gait cycle. As noted by Frimenko et al. [12], these latter variables are often more related to structure than motion,. Therefore a good interpretation of the data is required to be able to distinguish them. We decided to include central tendency measures because our purpose was to find structural and kinematic differences by gender. These measures allowed retrieval of the limb position inherited by gait pattern.

Our results showed clear evidence of differences by gender for hip ROM in the sagittal plane, with a greater value for women than men. Conversely, with a certified device and an entire population aged 50 years or older, Ko et al. [28] reported significantly lower hip ROM in the sagittal plane for women than men. According to Kobayashi et al. [29], gait pattern varies with age. In this context, with a younger population, Hurd et al. [30] reported greater hip ROM for women than men, but without significant difference. This could have been due to small study size, with only 20 participants. The most consistent results have been found for hip ROM in the frontal plane. Our results support earlier the theories of Bruening et al. [31], Cho et al. [24], and Hurd et al. [30]. They suggested a greater hip ROM in the frontal plane for women than for men. The same results were found even for the older adult population [28] and treadmill tests [32].

Ko et al. [28] analyzed knee excursion in the frontal plane, finding no significant differences by gender, though this study used an older adult population. With a similar sample to ours, both Cho et al. [24] and Roislien et al. [33] reported greater knee valgus angle in women than men. Similar results were found in our study. This could be an interesting difference linked to a potential cause for the prevalence of knee injuries in women.

FIGURE 8. The model performance evaluation. ROC curve for male and female classes.

The marker on the ROC curve (Fig. 8) shows the performance of the SVM classifier. The marker shows the values of the false positive rate (FPR) and the true positive rate (TPR). The FPR of 0.03 indicates that the SVM classifier assigns 3% of the observations incorrectly to the positive class. The TPR of 0.97 indicates that the SVM classifier assigns 97% of the observations correctly to the positive class. Similar results in ROC curve were achieved for both classes.

The area under curve (AUC = 0.99) is a measure of the overall quality of the SVM classifier. The maximum AUC is 1, which corresponds to a perfect classifier. Larger AUC values indicate better classifier performance.

The overall quality and accuracy of the chosen model represent very promising results to classify participants by gender using only depth sensors.

E. HIGHLIGHT FEATURES

In addition to the t-test applied, with the multivariate neighborhood component analysis (NCA), the highlights features to cluster both groups could be discovered. It can be seen in Fig. 9. Trunk rotation (Q75), trunk sway (IQR),

Cho *et al.* [24] reported a significant difference in the mean position value of pelvic tilt. Women had the pelvis tilted farther anteriorly. In addition, Chung *et al.* [34] reported the female trunk tilted farther anteriorly. These differences have been noted by gender in clinical measures of lower extremity alignment (LEA) [35]–[37]. According to [12], this is a manifestation of structural difference, rather than kinematics. Our central tendency and dispersion measures match these results. In addition, we found a significant difference in mean position for trunk sway, with greater value for men than women. This showed that women carry their trunk more centered, whereas men try to lean their body sideward. Furthermore, women had greater mean position of trunk and pelvic rotation (protraction or retraction). This could represent a strategy that women took to compensate their leg advance.

As we expected, there were differences revealed only in the frequency domain. Bruening *et al.* [31] reported that pelvic rotation has a possible phase shift. That study reported the concave external rotation wave was slightly delayed in women compared with men. This was only an empirical finding, without performing the phase shift analysis using a standard method. In contrast, through spectral analysis, we found no differences by gender in phase shift during pelvic rotation. However, an interesting significant difference was found in phase shift of knee flexion: women delay knee flexion, and therefore foot lift, compared with men. This could be due to anatomical differences, given women have shorter legs than men. To compensate for this difference, women try to get a more extended position of their knee. This allows women to achieve a higher advance with the opposite limb. No further differences were found when analyzing phase shift.

Pelvic obliquity has been proposed as a mechanism to lower VCOM excursions [38]–[40]. According to these authors, greater pelvic obliquity in women than men may represent a mechanism to reduce VCOM excursion. Consequently, this reduces energy consumption during walking. Smith *et al.* [40] used the sacrum as an estimated measure of COM excursion. The author showed that females had both greater pelvic obliquity and smaller VCOM excursion than males. These differences were found only for the older adult population. For a younger population, no significant differences were found. Bruening *et al.* [31] used the center of trunk segment as an approximation of the COM. The author reported significant difference only in normalized VCOM excursions, with greater values in women than men. Gomez Jiménez *et al.* [26] reported differences in non-normalized HCOM excursions, with lower values for women than men. In the latter case, the COM was chosen just anterior to the tenth thoracic vertebra as described by Perry and Burnfield [41]. We refute the COM position chosen in these previous studies. In contrast with them, we measured the COM position with regard to all body segments through the Winter method [27]. Our results showed that, although women had greater pelvic obliquity, there were no significant differences in vertical or horizontal COM excursions by gender. Similar results were found by [31].

Most strikingly, our results show clear evidence of gender differences in normalized COM position that match historical hypotheses. Results showed that men had a COM position higher than women, 51.7% versus 51.0% of their body height, respectively. Additionally, using the Winter method, we reported around 3 centimeters in VCOM and HCOM excursions. This is similar to older studies, which reported approximately 3–5 centimeters. Notably, measurement depends on sampling conditions.

Differences in the arm and shoulder have been less explored within analysis of the upper body. According to Bruening *et al.* [31], arm swing was higher in women compared to men. The author reported that the women had significantly greater shoulder ROM. Conversely, our system could not detect these differences. Only a difference in shoulder mid-position in the frontal plane was found. Although there were no significant differences, our results showed a lower shoulder ROM in the sagittal plane for women than men. The underlying reason could be related to gait speed. Gait speed has proven to have a significant effect on the movement of the upper limbs [42].

Frimenko *et al.* [12] reported that step length is related to body height and not related to gender. According to the author, height-matched participants of opposite gender likely have similar step lengths. Our results support this theory. As is indicated in [23], normalization by body height or leg length must be applied. In this way, no significant differences were found in step or stride length. Bruening *et al.* [31] had similar results for normalized measures. As mentioned earlier, women take different strategies to compensate for their lower leg length. Some of these strategies are related to delayed knee flexion and greater mean value of the trunk and pelvic rotation. Through these, women achieve a greater advance with the forward limb. These compensations could be the reason why gender differences in the normalized step or stride length disappear. Within step width, our results confirm a smaller normalized value when normalization by hip width is applied. This supports the theories of Gomez Jiménez *et al.* [26], Cho *et al.* [24], and Sakaguchi *et al.* [25], which employed a similar sample to ours.

Certain indicators were applied when choosing the dataset for this study to be representative of a young population. Kobayashi *et al.* [29] concluded that gait pattern is age-dependent, and Sun *et al.* [43] reported that different gait patterns related to self-esteem may exist between genders. According to the latter study, self-esteem levels look similar in young populations. These are the reasons that we focused our study only on a healthy young population with similar ages. This allowed us to avoid effects of health, age, or self-esteem on these measurements.

V. CONCLUSION

As we hypothesized, the proposed non-invasive, cost-effective system based on depth cameras may be able to retrieve relevant features of human gait patterns. We proved this by solving the problem of the classification of gait by gender.

Our results and classification performance also support the existing evidence about differences in gait pattern by gender.

Using the multivariate analysis NCA, the highlights features to cluster both groups were retrieved. Trunk rotation (Q75), trunk sway (IQR), knee abduction and adduction (entropy), and pelvic obliquity (ROM) were the features most differentiated between the groups.

In addition, earlier theories about the COM position, normalized spatial variables, ROM, and position of limbs during walking were supported. Central tendency measures allowed us to find many structural differences by gender. The magnitude of principal frequency measured the amount of movement at gait frequency and could be used as an alternative measure to ROM excursion. Finally, phase shift should be analyzed in more depth since no other studies were found with which to compare our results in detail.

In conclusion, these features could be used for a deeper biomechanical human gait analysis. It should be noted that the ankle excursion could not be detected, and the analysis of shoulder excursion produced opposite results to those reported in previous studies. These joints require special attention when being analyzed in the future. In addition, our future work will be to test how the system works in other environments. It will involve identifying walking patterns at different walking speeds, ages, or even for neurological diseases. The effectiveness of this kind of study helps to understand the importance of depth sensors for biomechanical assessments.

ACKNOWLEDGMENT

REFERENCES

[1] A. Muro-de-la-Herran, B. Garcia-Zapirain, and A. Mendez-Zorrilla, "Gait analysis methods: An overview of wearable and non-wearable systems, highlighting clinical applications," *Sensors*, vol. 14, no. 2, pp. 3362–3394, Feb. 2014. [Online]. Available: http://search.proquest.com/docview/1539402833/

[2] D. J. Geerse, B. H. Coolen, and M. Roerdink, "Kinematic validation of a multi-Kinect v2 instrumented 10-meter walkway for quantitative gait assessments," *PLoS ONE*, vol. 10, no. 10, Oct. 2015, Art. no. e0139913. [Online]. Available: http://search.proquest.com/docview/1721911213/

[3] S. Baek and M. Kim, "Dance experience system using multiple Kinects," *Int. J. Future Comput. Commun.*, vol. 4, no. 1, pp. 45–49, Feb. 2015.

[4] S. Li, P. N. Pathirana, and T. Caelli, "Multi-Kinect skeleton fusion for physical rehabilitation monitoring," in *Proc. 36th Annu. Int. Conf. IEEE Eng. Med. Biol. Soc.* Piscataway, NJ, USA: Institute of Electrical and Electronics Engineers, Aug. 2014, pp. 5060–5063.

[5] H. B. Du, Y. W. Zhao, J. D. Han, X. G. Zhao, Z. Wang, and G. L. Song, "Data fusion of human skeleton joint tracking using two Kinect sensors and extended set membership filter," *Zidonghua Xuebao/Acta Automatica Sinica*, vol. 42, no. 12, pp. 1886–1898, 2016.

[6] E. E. Stone and M. Skubic, "Unobtrusive, continuous, in-home gait measurement using the microsoft Kinect," *IEEE Trans. Biomed. Eng.*, vol. 60, no. 10, pp. 2925–2932, Oct. 2013.

[7] B. Ben Amor, A. Srivastava, P. Turaga, and G. Coleman, "A framework for interpretable full-body kinematic description using geometric and functional analysis," *IEEE Trans. Biomed. Eng.*, early access, Oct. 10, 2019, doi: 10.1109/TBME.2019.2946682.

[8] E. Dolatabadi, B. Taati, and A. Mihailidis, "An automated classification of pathological gait using unobtrusive sensing technology," *IEEE Trans. Neural Syst. Rehabil. Eng.*, vol. 25, no. 12, pp. 2336–2346, Dec. 2017.

[9] S. Springer and G. Yogev Seligmann, "Validity of the Kinect for gait assessment: A focused review," *Sensors*, vol. 16, no. 2, p. 194, Feb. 2016.

[10] B. F. Mentiplay, L. G. Perraton, K. J. Bower, Y.-H. Pua, R. McGaw, S. Heywood, and R. A. Clark, "Gait assessment using the Microsoft Xbox one Kinect: Concurrent validity and inter-day reliability of spatiotemporal and kinematic variables," *J. Biomech.*, vol. 48, no. 10, pp. 2166–2170, Jul. 2015.

[11] H. Lamine, S. Bennour, M. Laribi, L. Romdhane, and S. Zaghloul, "Evaluation of calibrated Kinect gait kinematics using a vicon motion capture system," *Comput. Methods Biomech. Biomed. Engin.*, vol. 20, no. sup1, pp. 111–112, 2017.

[12] R. Frimenko, C. Whitehead, and D. Bruening, "Do men and women walk differently? A review and meta-analysis of sex difference in non-pathological gait kinematics," Defense Tech. Inf. Center, Fort Belvoir, VA, USA, 2014, doi: 10.21236/ADA597428.

[13] L. Lee and W. E. L. Grimson, "Gait analysis for recognition and classification," in *Proc. 5th IEEE Int. Conf. Autom. Face Gesture Recognit.*, May 2002, pp. 155–162.

[14] A. M. C. B. Silva, J. R. R. da Cunha, and J. P. C. da Silva, "Estimation of pedestrian walking speeds on footways," *Proc. Inst. Civil Eng.-Municipal Eng.*, vol. 167, no. 1, pp. 32–43, Mar. 2014. [Online]. Available: http://search.proquest.com/docview/1528523556/

[15] P.-C. Su, J. Shen, W. Xu, S.-C. Cheung, and Y. Luo, "A fast and robust extrinsic calibration for RGB-D camera networks," *Sensors*, vol. 18, no. 1, p. 235, Jan. 2018. [Online]. Available: http://search.proquest.com/docview/2002811911/

[16] Z. Zhang, "A flexible new technique for camera calibration," *IEEE Trans. Pattern Anal. Mach. Intell.*, vol. 22, no. 11, pp. 1330–1334, Nov. 2000.

[17] J. S. Dai, "Euler–Rodrigues formula variations, quaternion conjugation and intrinsic connections," *Mechanism Mach. Theory*, vol. 92, pp. 144–152, Oct. 2015. [Online]. Available: http://www.sciencedirect.com/science/article/pii/S0094114X15000415

[18] M. Eltoukhy, J. Oh, C. Kuenze, and J. Signorile, "Improved Kinect-based spatiotemporal and kinematic treadmill gait assessment," *Gait Posture*, vol. 51, no. C, pp. 77–83, Jan. 2017.

[19] J.-C. Ceccato, M. de Sèze, C. Azevedo, and J.-R. Cazalets, "Comparison of trunk activity during gait initiation and walking in humans," *PLoS ONE*, vol. 4, no. 12, Dec. 2009, Art. no. e8193.

[20] V. Gavrishchaka, K. Davis, and O. Senyukova, "Multi-complexity measures for early detection and monitoring of neurological abnormalities from gait time series," in *Proc. AIP Conf.*, 2013, vol. 1559, no. 1, pp. 47–56.

[21] M. Zanin, D. Gómez-Andrés, I. Pulido-Valdeolivas, J. Martín-Gonzalo, J. López-López, S. Pascual-Pascual, and E. Rausell, "Characterizing normal and pathological gait through permutation entropy," *Entropy*, vol. 20, no. 1, p. 77, Jan. 2018. [Online]. Available: https://www.mdpi.com/1099-4300/20/1/77

[22] M. Li, S. Tian, L. Sun, and X. Chen, "Gait analysis for post-stroke hemiparetic patient by multi-features fusion method," *Sensors*, vol. 19, no. 7, p. 1737, Apr. 2019.

[23] A. L. Hof, "Scaling gait data to body size," *Gait Posture*, vol. 4, no. 3, pp. 222–223, May 1996.

[24] S. H. Cho, J. M. Park, and O. Y. Kwon, "Gender differences in three dimensional gait analysis data from 98 healthy korean adults," *Clin. Biomech.*, vol. 19, no. 2, pp. 145–152, Feb. 2004. [Online]. Available: http://www.sciencedirect.com/science/article/pii/S0268003303002389

[25] M. Sakaguchi, H. Ogawa, N. Shimizu, H. Kanehisa, T. Yanai, and Y. Kawakami, "Gender differences in hip and ankle joint kinematics on knee abduction during running," *Eur. J. Sport Sci.*, vol. 14, no. sup1, pp. S302–S309, Jan. 2014. [Online]. Available: http://www.tandfonline.com/doi/abs/10.1080/17461391.2012.693953

[26] M. G. Jiménez, C. de Subijana Hernández, and S. V. Fernández, "Comportamiento de la pelvis, el centro de gravedad y la cadera de hombres y mujeres durante la marcha normal," *Kronos Rev. Univ. La Act. Física Y El Deport.*, vol. 14, no. 2, p. 7, 2015. [Online]. Available: https://dialnet.unirioja.es/servlet/oaiart?codigo=5552527

[27] D. A. Winter, *Biomechanics and Motor Control of Human Movement*, 4th ed. Hoboken, NJ, USA: Wiley, 2009.

[28] S.-U. Ko, M. I. Tolea, J. M. Hausdorff, and L. Ferrucci, "Sex-specific differences in gait patterns of healthy older adults: Results from the baltimore longitudinal study of aging," *J. Biomech.*, vol. 44, no. 10, pp. 1974–1979, Jul. 2011. [Online]. Available: http://www.sciencedirect.com/science/article/pii/S002192901100371X

[29] Y. Kobayashi, H. Hobara, T. A. Heldoorn, M. Kouchi, and M. Mochimaru, "Age-independent and age-dependent sex differences in gait pattern determined by principal component analysis," *Gait Posture*, vol. 46, pp. 11–17, May 2016. [Online]. Available: http://www.sciencedirect.com/science/article/pii/S0966636216000321

[30] W. J. Hurd, T. L. Chmielewski, M. J. Axe, I. Davis, and L. Snyder-Mackler, "Differences in normal and perturbed walking kinematics between male and female athletes," *Clin. Biomech.*, vol. 19, no. 5, pp. 465–472, Jun. 2004. [Online]. Available: http://www.sciencedirect.com/science/article/pii/S0268003304000294

[31] D. A. Bruening, R. E. Frimenko, C. D. Goodyear, D. R. Bowden, and A. M. Fullenkamp, "Sex differences in whole body gait kinematics at preferred speeds," *Gait Posture*, vol. 41, no. 2, pp. 540–545, Feb. 2015. [Online]. Available: http://www.sciencedirect.com/science/article/pii/S0966636214007942

[32] E. S. Chumanov, C. Wall-Scheffler, and B. C. Heiderscheit, "Gender differences in walking and running on level and inclined surfaces," *Clin. Biomech.*, vol. 23, no. 10, pp. 1260–1268, Dec. 2008. [Online]. Available: http://www.sciencedirect.com/science/article/pii/S0268003308002295

[33] J. Røislien, Ø. Skare, M. Gustavsen, N. L. Broch, L. Rennie, and A. Opheim, "Simultaneous estimation of effects of gender, age and walking speed on kinematic gait data," *Gait Posture*, vol. 30, no. 4, pp. 441–445, Nov. 2009. [Online]. Available: http://www.sciencedirect.com/science/article/pii/S0966636209001957

[34] C. Y. Chung, M. S. Park, S. H. Lee, S. J. Kong, and K. M. Lee, "Kinematic aspects of trunk motion and gender effect in normal adults," *J. NeuroEng. Rehabil.*, vol. 7, no. 1, p. 9, 2010. [Online]. Available: https://www2.scopus.com/inward/record.uri?eid=2-s2.0-77949441717&doi=10.1186%2F1743-0003-7-9&partnerID=40&md5=e4d7995b3f80602a42eab7889c6b3e23

[35] J. Hertel, J. H. Dorfman, and R. A. Braham, "Lower extremity malalignments and anterior cruciate ligament injury history," *J. Sports Sci. Med.*, vol. 3, no. 4, p. 220, 2004.

[36] A.-D. Nguyen and S. J. Shultz, "Sex differences in clinical measures of lower extremity alignment," *J. Orthopaedic Sports Phys. Therapy*, vol. 37, no. 7, pp. 389–398, Jul. 2007.

[37] J. M. Medina McKeon and J. Hertel, "Sex differences and representative values for 6 lower extremity alignment measures," *J. Athletic Training*, vol. 44, no. 3, pp. 249–255, May 2009. [Online]. Available: http://search.proquest.com/docview/206649099/

[38] J. B. D. M. Saunders, V. T. Inman, and H. D. Eberhart, "The major determinants in normal and pathological gait," *J. Bone Joint Surg.*, vol. 35, no. 3, pp. 543–558, Jul. 1953.

[39] D. C. Kerrigan, P. O. Riley, J. L. Lelas, and U. D. Croce, "Quantification of pelvic rotation as a determinant of gait," *Arch. Phys. Med. Rehabil.*, vol. 82, no. 2, pp. 217–220, Feb. 2001. [Online]. Available: http://www.sciencedirect.com/science/article/pii/S0003999301598585

[40] L. K. Smith, J. L. Lelas, and D. C. Kerrigan, "Gender differences in pelvic motions and center of mass displacement during walking: Stereotypes quantified," *J. Women's Health Gender-Based Med.*, vol. 11, no. 5, pp. 453–458, Jun. 2002.

[41] J. Perry and J. Burnfield, *Gait Analysis: Normal and Pathological Function*, 2nd ed. Thorofare, NJ, USA: SLACK Incorporated, 2010.

[42] K. M. T. Goutier, S. L. Jansen, C. G. C. Horlings, U. M. Kung, and J. H. J. Allum, "The influence of walking speed and gender on trunk sway for the healthy young and older adults," *Age Ageing*, vol. 39, no. 5, pp. 647–650, Sep. 2010.

[43] B. Sun, Z. Zhang, X. Liu, B. Hu, and T. Zhu, "Self-esteem recognition based on gait pattern using Kinect," *Gait Posture*, vol. 58, pp. 428–432, Oct. 2017, doi: 10.1016/j.gaitpost.2017.09.001.

DIEGO GUFFANTI received the bachelor's degree in electronics, automation, and control from the Universidad de las Fuerzas Armadas (ESPE), in 2014, and the M.S. degree in electromechanical engineering from the Universidad Politécnica de Madrid (UPM), in 2017, where he is currently pursuing the Ph.D. degree in automatic and robotics, sponsored by the government of Ecuador. He is also collaborating with the Centre for Automation and Robotics (CAR), CSIC. His research interests include human gait analysis and machine learning.

ALBERTO BRUNETE (Member, IEEE) received the M.S. degree in telecommunication engineering and the Ph.D. degree in robotics and automation from the Universidad Politécnica de Madrid (UPM), in 2000 and 2010, respectively. He was the Technical Manager of the Research Center for Smart Buildings and Energy Efficiency (CeDInt), UPM, and a Visiting Professor with Carlos III University. He is currently an Associate Professor with UPM and a Researcher with the Centre for Automation and Robotics, UPM. His main research interests include service robots and smart environments. In 2016, he has received the Spanish prize ABC Solidario of a fall detector project for elderly people.

MIGUEL HERNANDO (Member, IEEE) received the M.S. degree in electrical engineering and the Ph.D. degree in automatic control and robotics from the Universidad Politécnica de Madrid (UPM), in 1997 and 2003, respectively. He has participated in several international and national research and development projects on robotics. He is one of the founders of the startup Biicode whose aim is to give (C/C++) to a dependency manager (currently Conan.io). He is currently a Professor with the Department of Electronics and Automatic Control, UPM, where he is also a Researcher with the Centre for Automation and Robotics (CAR), CSIC. His research interests include motion path planning, service robots, and micro-robotics.

• • •